Indian Journal of Chemistry
Vol. 59A, September 2020, pp. 1278-1284

Mechanism of photoinduced charge transfer at MEH-PPV and titanium dioxide nanoparticle interface

Jaya Seeli Shankar[a], Sangeetha Ashok Kumar[a], Bhuvana K Periyasami[b]* & Sanjay K Nayak[a]

[a]School for Advanced Research in Polymer (SARP) – ARSTPS, Central Institute of Plastics Engineering and Technology (CIPET), Chennai, Tamil Nadu, India
[b]Department of Plastics Technology, Central Institute of Plastics Engineering and Technology (CIPET), Chennai, Tamil Nadu, India
*E-mail: kpusha27@gmail.com

Received 18 April 2020; *accepted 26 July 2020*

In this study, we investigated mechanisms of photoinduced electron transfer from a conjugated polymer (poly(2-methoxy-5-(2-ethylhexyloxy) 1,4-phenylenevinylene (MEH-PPV) to titanium dioxide (TiO_2) nanoparticles (acceptor) through steady-state photoluminescence (PL) spectroscopy. Since mixed phase TiO_2 has better photocatalytic compared to single phase, it is an efficient charge separation process during photoexcitation of polymer nanocomposites by incorporating the mixed phase TiO_2 nanoparticles into the MEH-PPV polymer matrix through *in situ* polymerization. Structural characterization revealed only physical interaction between the polymer matrix and dispersed nanoparticles. The absorbance spectra of nanocomposites also indicated the absence of ground state complex formation. Luminescence quenching of polymer nanocomposites compared to pristine MEH-PVV signifies the charge transfer taking place at the MEH-PPV/TiO_2 interfaces. Thus, the MEH-PPV/ mixed phase TiO_2 nanocomposite serves as an active layer for photovoltaic application.

Keywords: Charge transfer, Conjugated polymer, Hybrid polymer nanocomposite (HPNC), Photoluminescence quenching, Photovoltaics

Hybrid polymer nanocomposites (HPNCs) are prepared by combining organic conjugate polymer with inorganic semiconductor nanoparticles. These have been an object of great attention in the field of optoelectronic devices. This combines the processability of organic material with the superior electrical conductivity and stability of inorganic nanoparticles[1]. The basic requirement of a photovoltaic material is to generate free charge carriers under photoexcitation. But the major drawbacks of using conjugated polymers in photovoltaics is short exciton diffusion length (5-20 nm)[2] and the trap limit electron transfer caused by single oxygen radical scavenger, water molecules, halogens and defects in the polymeric chain due to photo oxidation[3]. Hence, the limitations are overcome by inclusion of high electron affinity substance, such as fullerene derivative phenyl-C61 butyric acid methyl ester (PCBM)[4] or nanoparticle (ZnO, TiO_2)[5,6]. Among them, nanoparticles are considered to be more attractive owing to their large surface-to-bulk ratio, giving an extension of interfacial area for electron transfer, and higher stability. Nanoparticles contained in the polymer layer acts as dopants and increases the charge carriers and conductivity, thereby influence the optoelectronic properties of final device application[7] for different uses[8,9].

In the case of photovoltaics, the charge separation process must be fast compared to radiative or non-radiative decays of the singlet exciton[4]. However, electron transport in the polymer/nanoparticle interface is usually limited by poorly formed conduction path. Hence, in bulk heterojunction, the morphology and the domain sizes of the polymer phase should be comparable to the diffusion length of the excitons for effective charge transfer at the interface. Both polymer and nanoparticle phases have to be continuous for effective charge transport[6]. Therefore, the present study proposes the *in situ* polymerization of α,α'–dibromo-2-methoxy-5-(2-ethylhexyloxy) benzene into poly (2-methoxy,5-(2'-ethyl-hexyloxy)-p-phenylenevinylene) — MEH-PPV in the presence of titanium dioxide (TiO_2) nanoparticles to form HPNCs. The uniqueness of this work lies in the fact of utilizing the mixed phase TiO_2 nanoparticles to prepare HPNCs. Generally, in case of formulating a HPNCs using TiO_2 nanoparticles, anatase phase TiO_2 is preferred compared to rutile or brookite[10] owing to its wider band gap (3.2 eV), lower rates of recombination (10 fold higher hole trap compared to rutile) and higher surface adsorptive capacity[11]. But in the mixed phase TiO_2, the migration of electrons and holes, because of the difference valance band and conduction band, makes it superior than the anatase TiO_2. The enhanced activity of mixed phase TiO_2 relative to pure phases was due the transfer of electrons from lower energy rutile to anatase which acts as electron trapping site leading efficient electron-hole separation making it a suitable candidate for photovoltaics[12].

Usually the nanoparticles tend to agglomerate and phase separate during the formation of bulk heterojunction leading to poor device performance[1]. To resolve the agglomeration problem and enhance the interaction between MEH-PPV and TiO_2, the prepared TiO_2 nanoparticles were ultrasonicated with α,α'–dibromo-2-methoxy-5-(2-ethylhexyloxy) benzene (monomer of MEH-PPV) followed by polymerization. Thus, incorporation of nanoparticles into the polymer matrix introduce new energy states which can mediate the electron transport from LUMO of MEH-PPV to the conduction band of TiO_2 nanoparticles under photoexcitation. Consequently, the two major drawbacks of short exciton diffusion length of MEH-PPV (~14 nm) and low electron mobility were suppose to overcome by intermixing of materials with high electron affinity in MEH-PPV using insitu polymerization. (χ of TiO_2 – 4eV; χ of MEH-PPV – 3eV).

Materials and Methods

Synthesis of TiO_2 nanoparticles

TiO_2 nanoparticles were prepared by sol-gel method as described. 1.0 mL of titanium tetrachloride ($TiCl_4$) was slowly added to the 10% diluted sulfuric acid solution at 0ºC under constant stirring for about 30 min. During this process, white fume of HCl was released as a consequence of the reaction between $TiCl_4$ and H_2SO_4 resulting in the formation of a grey coloured solution. This grey solution was heated at 60ºC until a clear solution was obtained which was left undisturbed for 12 h for cooling. Later NaOH was added dropwise to the above solution until pH =7 was attained (neutralization process) where the solution transformed to a white colour solution followed by gelation period of 12 h. The precipitate formed was filtered and washed twice with distilled water. Later the filtrate was calcined at 600ºC for two hours to acquire TiO_2 nanopowder. The product obtained was grinded into a fine powder using mortar and stored in a desiccators until further usage.

$$TiCl_4 + 2H_2SO_4 \rightarrow Ti(SO_4)_2 + 4HCl$$

$$Ti\,(SO_4)_2 + 4NaOH \rightarrow Ti(OH)_4 + 2Na_2SO_4$$

$$Ti(OH)_4 \rightarrow TiO_2 + 2H_2O$$

Synthesis of MEH-PPV

Poly 2-methoxy-5-(2'-ethylhexyloxy-p-phenylene vinylene) (MEH-PPV) was prepared by the well know glich route process[13] through solution polymerization technique in a course of three stages of reactions. First step involves the preparation of 1-methoxy-4-(2-ethylhexyloxy) benzene (MEHB – labeled as Monomer-1) from the base materials P-methoxyphenol (PMP) and 2-ethylhexyl bromide. Then α,α'–dibromo-2-methoxy-5-(2-ethylhexyloxy) benzene (MEH-DBMB – labeled as Monomer-2) was prepared through bromination of MEHB. Finally, polymerization of MEHDBMD yields Poly 2-methoxy-5-(2'-ethylhexyloxy-p-phenylene vinylene) (MEH-PPV). The synthesis procedure was reported elsewhere[14] and the schematic diagram of the reaction is given in Scheme 1.

Preparation of MEH-PPV/TiO_2 nanocomposite

The TiO_2 incorporated polymer nanocomposites were synthesized through *in situ* polymerization represent in flow diagram (Scheme 2). The α,α'–dibromo-2-methoxy-5-(2-ethylhexyloxy) benzene – MEHDBMB (monomer of MEH-PPV) was dissolved in Tetra-hydrofuran (THF). The TiO_2 nanoparticles were dispersed in the MEHDBMB solution with different loading concentrations of 1, 3 and 5 wt.% with respect to weight of MEHDBMD.

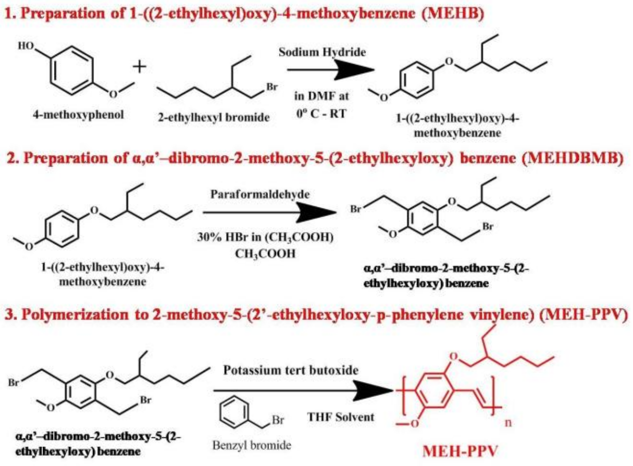

Scheme 1 — Reaction Scheme of MEH-PPV preparation

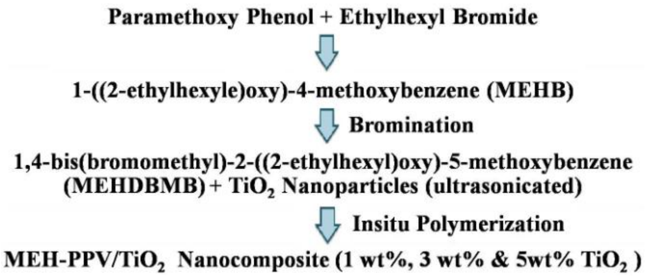

Scheme 2 — Flow chart for the preparation of HPNCs

Polymerization of 300 g MEHDBMB (monomer-2) with TiO_2 content was carried out in 30 mL THF solution with 2 g potassssium tert butoxide (t-BuOK) as the catalyst. To this reaction mixture, 60 mg of benzyl bromide (chain stopper) was added to prevent gelation. The reaction mixture was refluxed in N_2 atmosphere at 68°C for 3 h. The reaction product was precipitated by adding 40 mL methanol and filtered after reaching room temperature. The filtrate was washed with distilled water until pH 7 was attained, followed by 3 times washing with 20 methanol. The precipitate was dried in vacuum oven for 12 h. Deep red MEH-PPV/TiO_2 hybrid nanocomposites were obtained and subjected to structural and photophysical characterization to analyze the effect of nanoparticle interaction with conjugated polymer.

Characterization of hybrid nanocomposite

Fourier transformed infrared (FTIR) spectra were recorded using Nicolet iS5-6700 under ATR condition at wavenumber ranging from 4000 cm^{-1} to 500 cm^{-1}. X-ray diffraction (XRD) pattern were obtained using Rigaku Mini Flex X-ray diffractometer model using a monochromatic copper radiation (CuK_α) of wavelength $\lambda = 1.54$ Ǻ in the range of 20-80° with the step size of 0.02°. TiO_2 nanoparticles were dispersed in 5 mL distilled water through ultrasonication for 30 min and the particle size distribution was measured using MALVERN particle size analyzer under ambient condition with a count rate of 172 kcps. SEM micrographs were obtained from Field Emission Scanning Electron Microscopy (FESEM) - FEI Quanta 200 Model SEM. The photophysical characterization of all the materials was studied through UV-visible absorption spectra recorded using Cary 500 Scan model made by VARIAN, with wavelength ranging from 200 to 700 nm and Photoluminescence (PL) emission spectra in the wavelength ranging from 200 to 1100 nm recorded on a Cary Eclispe mode made by VARIAN using xenon pulse lamp as the source in ambient condition.

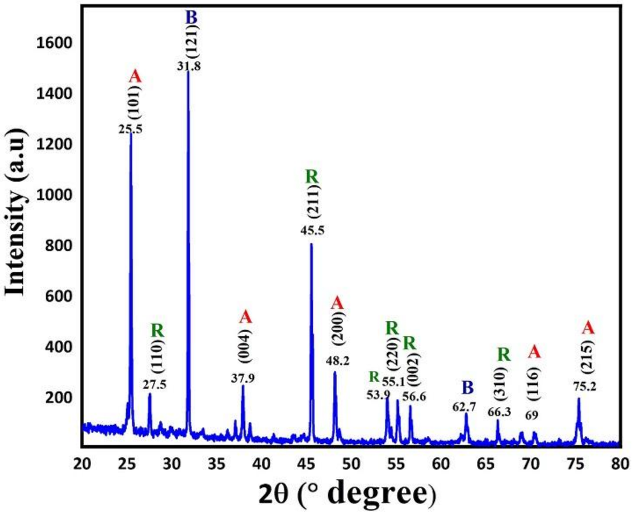

Fig. 1 — X-ray diffraction pattern of TiO_2 nanoparticles

Results and Discussion

Characteristics of TiO_2 nanoparticles

Structural characterization

Fig. 1 displays XRD patterns of synthesized TiO_2 nanoparticles. The prepared TiO_2 constitutes of mixed phase of tetragonal anatase (represented by A) and rutile (represented by R) along with traces of orthorhombic brookite (represented by B) which was in agreement with the data reported in the databases cards JCPDS no. 00-021-1272, JCPDS no.00-021-1276 and JCPDS no.00-029-1360, respectively. The diffraction peaks at 25.3°, 37.9°, 48.2°, 55.1°, 62.7° revels the anatase phase of TiO_2 nanoparticles. The diffraction peaks at 27.5°, 45.5°, 53.9°, 66.3° and 69° indicating the rutile phase of TiO_2[12]. In the phase composition of TiO_2, an additional peak at 30.8° confirms the fraction of brookite phase arises due to decrease in pH during synthesis[15]. Addition of NaOH had favoured the formation of rutile. Generally, the higher surface energy has contributions to non-equlibirium transition from anatase to rutile which was facilitated by calcining at 600°C[16]. But it was observed that the incorporation of sulfate ion during the synthesis stabilized the anatase phase, inhibiting the prominent formation of the rutile phase[15]. The proposition of anatase/rutile phase composition can be estimated using the Spurr and Myers equation[17]:

$$f = \frac{1}{1+1.26\frac{I_R}{I_A}}$$

Where, I_R and I_A are the peak area of diffraction peaks of rutile (110) and anatase (101), respectively. From the above equation the anatase to rutile proportion was estimated as ~83%. The XRD studies revealed the formation of mixed phase TiO_2 with predominant orientation in anatase phase.

Morphological studies: SEM and particle size analysis of TiO_2 nanoparticles

The SEM micrographs of TiO_2 nanoparticles at 25 kX magnification (Fig. 2A) show that the particles are spherical with an average diameter of 140 nm; and crystalline in nature with defined grain boundaries. The particles are agglomerated owing to the high surface energy of TiO_2 nanoparticles which is observed from the SEM images. Fig. 2B displays the size distribution of TiO_2 nanoparticle which covers the range from 150 to 250 nm with the average size of 189 nm. A small hump around 280 nm denotes the agglomerates.

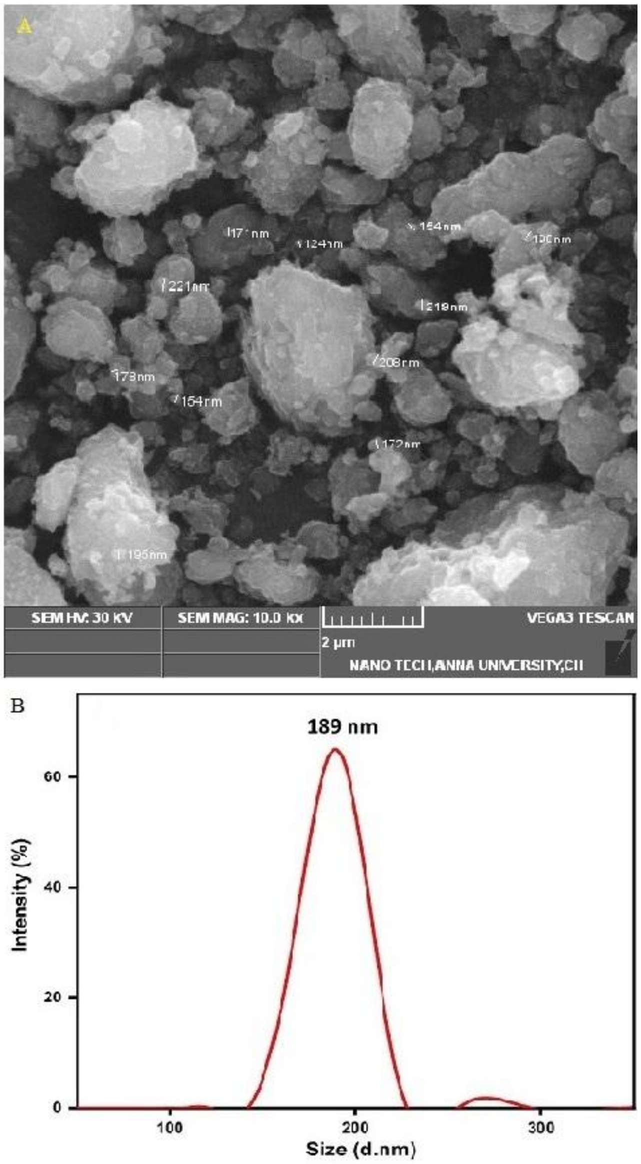

Fig. 2 — (A) SEM image at 25 kX magnification and (B) particle size analysis graph of TiO_2 nanoparticles

Characteristics of MEH-PPV/TiO_2 hybrid nanocomposite

Structural characterization

Fig. 3 shows the FTIR spectra of MEH-PPV, TiO_2 and MEH-PPV/TiO_2 nanocomposites. The FTIR spectrum of MEH-PPV [Fig. 3(i)] denotes the main characteristic absorption bands at 2957, 2856 and 2924 cm^{-1} band of CH_3, CH_2 asymmetrical and C-H stretching vibrations, respectively. Three semicircular stretch bands associated with the phenyl ring are observed at 1408, 1501 and 1606 cm^{-1}. The other vibration at 863 and 965 cm^{-1} indicates out of plane phenyl CH wag and trans double bond C-H wag. Symmetrical and asymmetrical C-O-C stretching vibration modes are located at 1032 and 1202 cm^{-1}, respectively corresponds to alkyl oxygen stretch and phenyl oxygen stretch. The small band at 1736 cm^{-1} could be attributed due to the carbonyl absorption. The 1460 and 794 cm^{-1} shows band of CH_3 asymmetrical C-H bending and mono substituted aromatic ring C-H bending[14]. The band at 1447 cm^{-1} corresponds to O-H bending vibration of water. Ti-O-Ti vibration bonds were found at 875 cm^{-1}. The peak observed at 1102 cm^{-1} corresponds to the C-O vibration. The band at 609 and 635 cm^{-1} could be attributed to the stretching mode of Ti-O bonds,

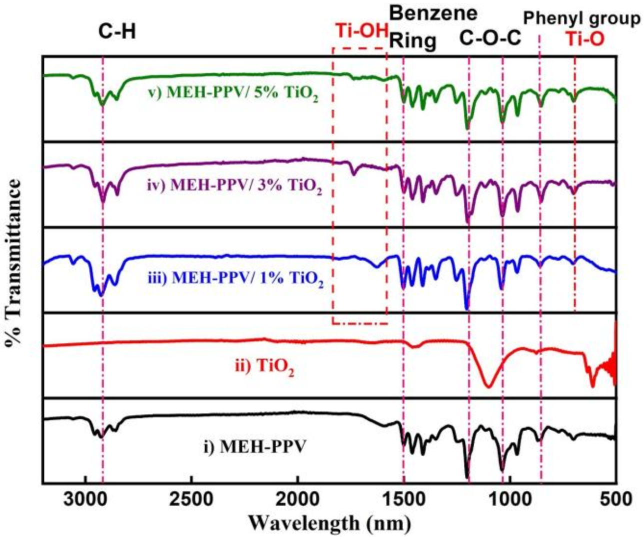

Fig. 3 — FTIR spectra of MEH-PPV and MEH-PPV/TiO_2 nanocomposites

which are characteristic of titanium oxide. The FTIR spectra of hybrid nanocomposite were similar to that of MEH-PPV. Since TiO_2 was incorporated in a very low quantity, there is no significant change in the FTIR spectra was observed in the nanocomposites. The presence of additional bands at 1650-1700 cm^{-1} denotes the Ti-OH bond. The band around 856 cm^{-1} signifies the presence of TiO_2 nanoparticles. Thus, the presence of the nanoparticles in the composites was confirmed.

The XRD studies of the nanocomposite were carried out in order to examine the influence of TiO_2 nanoparticles into the MEH-PPV polymer. Fig. 4 shows the XRD pattern of MEH-PPV/TiO_2 nanocomposite. It is evident from Fig. 4(i) that the pristine MEH-PPV polymer with a broad peak at $2\theta = 22^o$, is highly amorphous in nature. Similarly, the diffraction peak of polymer nanocomposites displayed the broad peak at ~22º with a slight peak shift due to the internal stress induced by the addition of TiO_2 nanoparticles into the polymer matrix. Due to trace amount of TiO_2 dispersion the diffraction peaks of the nanoparticles were not distinct in XRD of polymer nanocomposites. But in Fig. 4(iii), a low intensity peak at 26.8º denotes TiO_2. This might be due the improper dispersion of TiO_2 nanoparticles in the polymer nanocomposites which tends to agglomerate and became visible during analysis.

Photophysical characterization

HPNC thin films were obtained by dissolving HPNCs in toluene at a concentration of 10 mg/mL. This solution was spin coated on to a cleaned glass substrate at a speed of 1500 rpm for 5 times at 35°C to obtain approximately 1 μm thick film for PL studies.

The absorbance and emission spectra of MEH-PPV and MEH-PPV/TiO2 nanocomposites are given in Fig. 5 A & B. Both MEH-PPV and the nanocomposite exhibit a broad absorbance peak centered at ~490 nm is attributed to the π–π* transition of the conjugated polymers. No evidence of any additional peak in the measured spectral region denotes the absence of ground state complex which implies that there is no formation of any new complex species with the addition of TiO_2 in MEH-PPV. When the thin films of MEH-PPV and hybrid nanocomposite were excited at 480 nm, the emission spectra of hybrid nanocomposite films were similar to that of the pristine MEH-PPV. However, the decrease in PL intensity was observed as the TiO_2 content increases since the film was coated in same condition and at the same concentration of solution. The decreased intensity could be due to the quantity of TiO_2. On examining the emission spectra, it can be seen that the luminescence primarily results from the excitons

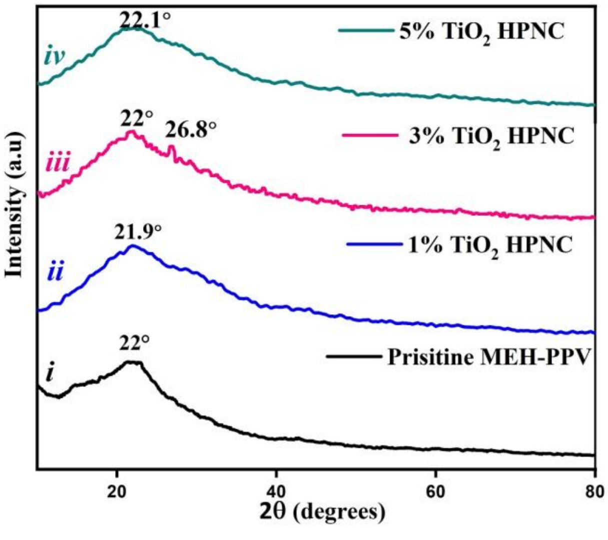

Fig. 4 — XRD patterns of MEH-PPV and MEH-PPV/TiO_2 nanocomposites

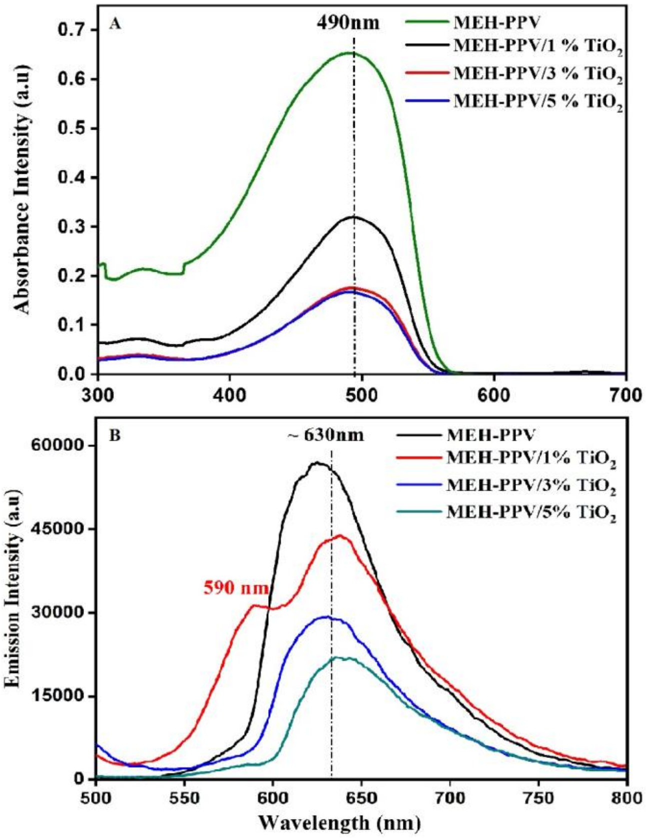

Fig. 5 — (A) Absorbance and (B) emission spectra of MEH-PPV and MEH-PPV/TiO_2 nanocomposites

which radiatively recombine in MEH-PPV. A predominant peak at 630 nm is attributed to the interchain excitons of MEH-PPV, since the thin films were obtained from the solution of higher concentration. A small hump at 590 nm in the case of 1% TiO_2, HPNC film signified the presence of intrachain excitons of MEH-PPV in a minimal quantity. This was owing to the fragmentation of few polymer chains through addition of nanoparticles. Nevertheless, the intensity of the PL emission (630 nm) in the composites decreasing substantially with increasing TiO_2 nanoparticle content denotes the charge separation occurring at the interface of the luminescent polymer and nanoparticle which is responsible for the photoluminescence quenching[18]. The charge separation at the interface is on the basis of relative energy levels of MEH-PPV and TiO_2 nanoparticles where the disassociation of the excitons is energetically allowed. Due to better PL quenching and enhanced charge transfer these hybrid nanocomposites are expected to be useful in photovoltaic applications[4].

Charge Transfer Process from MEH-PPV to mixed phase TiO_2

An electron and hole that is coulombically bound is termed as an exciton. A charge separation can take place only when the binding energy is overcome which is done by photoexcitation of the conjugated polymer. Such a charge separation can be made efficient with a material with higher electron affinity and only if the LUMO level of polymer is lower than Conduction band of the semiconductor metal oxide where the polymer acts as donor and metal oxide as an electron accepting material. Additionally, there should not be much potential difference between both donor and acceptor. A short range interaction brings about spatial over lap of wavefunction of donor and acceptor; as a result disassociation of exciton takes place significantly at the polymer/nanoparticle interface. Moreover, the interface between the polymer and the nanoparticle plays a crucial role in determining the performance of the device. Hence intermixing with the polymer at the nanometer scale for efficient charge transfer is achieved in this case. anatase phase has more electron affinity, hence mixed phase TiO_2 which was predominantly in anatase phase had facilitated efficient separation of photogenerated electrons from MEH-PPV. In this process, the rutile phase has lower conduction band compared to anatase supported in initial extraction of electrons from MEH-PPV. The electron in rutile is transferred to anatase phase which facilitates movement of electrons further away from MEH-PPV which inhibits the recombination process. Hence, the mixed phase TiO_2 acts as an efficient quencher for MEH-PPV and therefore, the MEH-PPV/TiO_2 can be a suitable active layer in photovoltaics. The process of charge transfer from MEH-PPV to mixed phase TiO_2 is represented in the Fig. 6.

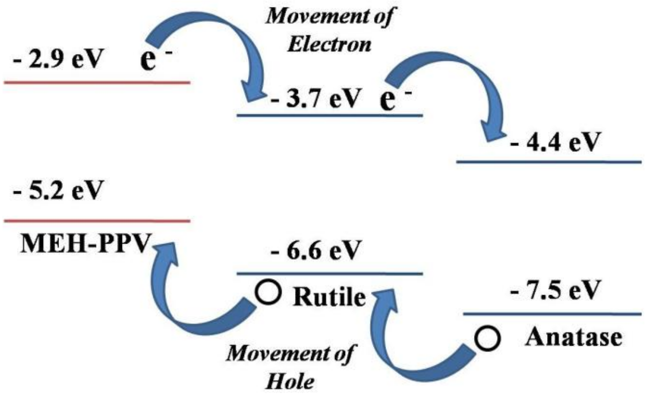

Fig. 6 — Charge Transfer prccess between MEH-PPV and mixed Phase TiO_2

Conclusions

The results of the analysis of photoinduced charge transfer from MEH-PPV to the mixed phase TiO_2, particularly the steady state PL measurements, reveal remarkable quenching of luminescence with increased TiO_2 content. The luminescence quenching was due to the transfer of photogenerated electrons from the polymer to TiO_2. Structural analysis indicates that the chemical structure of the polymer remains unaffected by the incorporation of TiO_2 nanoparticles. In summary, the new approach of incorporation of mixed phase TiO_2 nanoparticles through *in situ* polymerization in the conjugated polymer matrix has resulted in efficient charge separation. Hence, this type of polymer nanocomposites is a suitable candidate for photovoltaic applications as active layer.

Acknowledgement

The authors are thankful to the Council for Scientific and Industrial Research (CSIR), New Delhi for their financial support to carry out the project.

Conflict of interest

The authors declare no conflict of interests in this study.

References

1 Li S, Lin M M, Toprak M S, Kim D K & M. Muhammed M, *Nano Rev*, 1 (2010) 1.

2 Kousal J, Kindl D & Kur I, *Chem Phys*, 552 (2012) 49.

3 Abbaszadeh D, *Chem Mater*, 31 (2019) 6380.

4 Lin Y, *Nanotechnology*, 17 (2006) 5781.

5 Jetson R, Yin K, Donovan K & Zhu Z, *Mater Chem Phy*s, 124 (2010) 417.

6 Petrella A, Tamborra M, Curri M L, Cosma P, Striccoli M, Cozzoli P D & Agostiano A, *J Phys Chem B*, 109 (2005) 1554.

7 Choi Y, Park H, Golledge S & Johnson DC, *Ceram Int*, 38 (2012) 525.

8 Balakrishnan T & Murugan E, *J Polymer Sci A*, 41 (2003) 347

9 Murugan E, Gopinath P, Shanmugayya V & Mathivanan N, *J Appl Polym Sci*, 117 (2010) 3673.

10 Petrella A, Tamborra M, Cozzoli PD, Curri ML, Striccoli M, Cosma P, Farinola GM, Babudri F, Naso F & Agostiano A, *Thin Solid Films*, 452 (2004) 64.

11 Hurum DC, Agrios AG, Gray K A, Rajh T & Thurnauer MC, *J Phys Chem B*, 107 (2003) 4545.

12 Lei S H & Duan W, *J Enviorn Sci*, 20 (2008) 1263.

13 Neef CJ & Ferraris JP, 33 (2000) 2311.

14 Shankar J S, Kumar S A, & Periyasamy B K, 2559, 2018.

15 Benito H E, Sánchez T D A, Alamilla R G, Hernández J M & Robles G S, *Brazilian J Chem Eng*, 31 (2014) 737.

16 Mahshid S, Askari M, Ghamsari M S, Afshar N, & Lahuti S, *J Alloys Compd*, 478 (2009) 586.

17 Spurr R A & Myers H, *Anal Chem*, 29 (1957) 760.

18 Ton-that C, Phillips M R & Nguyen T, *J Lumin*, 128 (2008) 2031.